

TURBINE AIRFOIL DEPOSITON MODELS AND THEIR HOT CORROSION IMPLICATIONS*

D.E. Rosner and R. Nagarajan

Yale University

Department of Chemical Engineering

High Temperature Chemical Reaction Engineering Laboratory

1. INTRODUCTION

Gas turbine failures associated with sea-salt ingestion and sulfur-containing fuel impurities have directed attention to alkali sulfate deposition and the consequent 'hot corrosion' of gas turbine (GT) blades under some GT operating conditions. These salts deposit and form thin, molten films which undermine the protective metal oxide coating normally found on GT blades. This research project deals with the prediction of single- and multi-component salt(-solution) deposition, flow and oxide dissolution and their effects on the lifetime of turbine blades. Our goals include rationalizing and helping to predict corrosion patterns on operational GT rotor blades and stator vanes, and ultimately providing some of the tools required to design laboratory simulators and future corrosion-resistant high-performance engines. In the program summary that follows we first review necessary background developments (Section 2) and then outline our results and tentative conclusions for single-species ($\text{Na}_2\text{SO}_4(l)$) condensation (Section 3), binary salt-solution ($\text{Na}_2\text{SO}_4\text{-K}_2\text{SO}_4$) condensation (Section 4), and burner-rig testing of alloy materials (Section 5). We conclude with a brief account of our research plans (Section 6) should follow-on funding become available.

2. THEORY OF CONDENSED LAYER FORMATION AND FLOW

The necessary first step in a complex sequence of events leading to hot corrosion failures is the deposition of alkali salts from the combustion products onto turbine blades and vanes. Our NASA-supported laboratory experiments (refs. 1, 2, 3, 4), and those carried out in collaboration with the NASA-Lewis Research Laboratories (ref. 5) have enabled further advances in salt deposition rate theory, as outlined here. A comprehensive but tractable method for predicting the rates of chemical vapor deposition (CVD) of, say, alkali sulfates from multicomponent salt-laden combustion gases has been developed, illustrated and tested in part (refs. 5, 6, 7). This theory, based on vapor diffusion through a 'chemically-frozen' (CF) gas boundary layer (BL), predicts important effects of multicomponent diffusion and thermal (Soret) diffusion (ref. 8) on dew points, CVD-rates and deposit compositions (ref. 9). A reference manual prepared for NASA-LeRC by GOKOGLU et al. (ref. 10) provides information on the structure of a CFBL computer program for the calculation of convective diffusion deposition rates, and details regarding the program input and output. Our CFBL-VD approach also applies without fundamental modifications to the deposition of pre-existing fine particles (refs. 11, 12). The inclusion of chemical reactions and/or phase change (e.g., 'mist

*Work done under NASA Grant NAS3-590.

formation') within the BL is the subject of ongoing research at the Yale HTRC laboratories (refs. 13, 14, 15).

'Fluxing' of the oxide layer by the molten salt-'solvent' can occur only in the presence of dynamic processes which allow dissolution to proceed without locally saturating the liquid layer. For this reason, we have carried out studies of the dynamics of thin condensate layers, allowing for the interplay of salt arrival and run-off induced by the gas-dynamic shear-stress, $\tau_{w,g}$, and blade rotation (with velocity Ω) (fig. 1). Earlier (ref. 16), the necessary liquid layer theory was developed and used to predict steady-state laminar single-component condensate layers on smooth, non-rotating isothermal targets, with emphasis on the circular cylinder in high Reynolds number cross-flow (a common test-configuration). Subsequently, this approach has been extended to include the treatment of single-component and binary-solution condensate layers on smooth non-isothermal turbine blades (refs. 17 and 18).

Illustrative calculations have thus far been made for a test turbine (NASA TP 1018 (1977)) but most of our methods will carry over to operational engine vanes and blades (except in the vicinity of cooling holes/slots). From the inviscid stream velocity data, we compute, using efficient integral methods, the corresponding distributions of gas-side momentum-, heat-, and mass-transfer coefficients, and the distribution of blade recovery temperature (used to estimate this root-cooled temperature distribution). The corresponding local salt arrival rates and liquid-phase physical properties are then inserted into the partial differential equations (PDE's) governing the evolution of quantities of engineering interest (QOI), such as the liquid layer thickness, $\delta_1(x,z)$ (fig. 1). The nonlinear first-order PDE's are numerically solved (by the method-of-characteristics) to obtain the condensate layer streamline pattern (fig. 2), as well as values of δ_1 , the salt arrival rate, $\dot{m}''(x,z)$, oxide bulk mass fraction in liquid, $\omega_{o,b}(x,z)$, and oxide dissolution rate, $j_{o,w}''(x,z)$. Important by-products of these calculations are estimated line- and surface-integral quantities, such as the steady-state salt inventory on the blade and relative tip and trailing edge (TE) run-off rates.

3. SINGLE-SPECIES CONDENSATE LAYERS ON GT BLADES

Representative calculations carried out by applying the above-mentioned formulation for $\text{Na}_2\text{SO}_4(1)$ layers on GT rotor blades have been reported in previous HOST conferences, and summarized in Reference 17. These include the generation of solute diffusion-limited dissolute rate distributions (fig. 3) associated with solvent flow patterns of the type shown in Figure 2. Our original intention of comparing relative oxide dissolution rate (RODR) 'maps' obtained in this manner with hot corrosion rate patterns observed on blades removed from operational GT engines has been set aside due to the unavailability of high-quality operational data. Our recent efforts have been directed towards investigating certain observed 'overall' trends. For instance, limited available results for operational engines indicate that hot corrosion rates are much larger on the pressure surface of GT blades than on the suction surface. An important question, addressable via our present model, is whether this can be explained on the basis of our CVD-oxide dissolution theory, or whether it is necessary to invoke particle impaction (refs. 12 and 19) on the pressure surface. Indeed, we found that in the limiting case of transverse heat equilibration across a solid blade, when the

blade is operating under feed and stagnation conditions such that every location on the blade surface is near the local dew point, the pressure-to-suction surface dissolution rate ratio is very large, tending to infinity in the limit of zero net-deposition on the suction surface (fig. 4). Another apparent anomaly that may now be rationalized on the basis of our theory has to do with liquid deposits observed by investigators to be present on some metal surfaces that are hotter than the local dew-point. This is a less-obvious but natural consequence of flow-induced liquid 'spill-over' onto evaporation regimes of blade surfaces (fig. 5).

Our comprehensive physico-chemical/mathematical model offers the potential of economical parametric studies. We have initiated such studies to gain an understanding of how turbine blade corrosion rates might respond to changes in parameters at the disposal of designers and engine-operators, or parameters which might vary due to local environmental changes (e.g., sea-salt ingestion at higher than anticipated levels). The material leaving the blade at the TE influences downstream stage/blade condensate flow-characteristics; a study of TE salt run-off is thus necessary to understand and solve the overall problem of hot corrosion in multi-stage turbines. The parametric dependency of the TE run-off rate (with pressure level and salt seed-level the variables being changed) is displayed in Figures (6) and (7).

4. BINARY CONDENSATE LAYER EFFECTS

All properties of thin liquid condensate films, including their aggressiveness as corrodants, are expected to be composition-dependent. Moreover, appreciable amounts of 'adulterants' (e.g., Ca- and Mg-compounds) are often found in GT blade deposits. This information, combined with the remarkable effect (observed at the Yale HTCRC labs.) the addition of a second salt can have on the deposition rate of the primary salt (ref. 4), directed our attention toward the deposition, dynamics and dissolution rate properties of multicomponent salt layers.

Among the effects observed for binary salt solutions, perhaps the most significant are the alteration of:

- (a) deposition rates and associated dew-point temperatures,
- (b) liquid properties, including oxide solubility and associated solute diffusivity, and
- (c) freezing point of the solution (the information being extracted from the relevant thermodynamic phase diagram).

While the property effects (b) are relatively minor for physically- and chemically-similar molten salts, effects (a) and (c) can considerably broaden the 'dangerous' temperature interval ($T_{dp} - T_{mp}$) within which hot corrosion is known to occur. To illustrate the consequences of the altered freezing-point we performed a preliminary steady-state analysis of the binary ($K_2SO_4 + Na_2SO_4$) layer condensing on the leading edge (LE) of a root-cooled rotor blade. Figure 8 reveals that with increasing potassium levels, an increasing fraction of the condensate would become molten, eventually becoming molten over the entire LE. Figure 9 shows a typical distribution of liquid phase composition over the suction surface of a rotor blade ($[K]/[Na] = 0.1$; $\Omega = 6786$ rad/s); the primary effect of shear- and centrifugally-driven flow here is to 'shift' the condensate composition from its local 'quasi-steady' value when the liquid flow rate becomes sufficiently high.

An examination of the Na_2SO_4 - K_2SO_4 binary phase-diagram suggests that

when the second component, K_2SO_4 , is in sufficient excess, the solution freezing point is actually raised above that of pure Na_2SO_4 . The evolution of the solution 'freezing-point locus' over the suction surface of a root-cooled rotor blade with changing values of the salt seed-ratio, $[K]/[Na]$, is depicted in figure 10. Upstream seeding techniques could conceivably be resorted to in order that a relatively-benign overlayer of solid sulfate 'ice' may deposit over the entire blade surface. It should also be borne in mind that increasing the amount of the second salt enhances the possibility of BL-phase change phenomena (fig. 11), which would reduce the net salt arrival rate.

5. SIMULATION CRITERIA FOR HOT CORROSION RIG-TESTING

There exists at present no standard testing procedure for determining the hot corrosion resistance of turbine blade alloy materials. Economic considerations and the requirement of a controllable environment have led to the development of two general types of laboratory procedures, one involving burner rigs and the other involving furnaces. Not surprisingly, burner rig testing appears to give a more realistic simulation of service behavior. The fundamental question of which aspect(s) of the turbine environment- the convective flux of the gas-phase contaminant, the salt-contaminant dew-point and deposition rate, the thicknesses of the liquid deposit layer and the protective oxide layer, the rate of dissolution of the oxide coating, the alloy composition, etc.- is/are most crucial in determining the system corrosion characteristics remains to be settled. We offer no conclusive argument in this regard, but point out that the required operating conditions of the test rig will be quite different depending on the investigator's choice of one or more of these parameters as being corrosion rate-controlling.

In a typical simulation procedure, the seed level and pressure level are compensatingly changed to reproduce the engine alkali sulfate dew-point in the atmospheric-pressure rig (fig. 12). Our stagnation line calculations for the GT rotor blade indicate that under equivalent dew-point conditions, the Mach number of gas flow, Ma_∞ , and hence the contaminant flux rate, have to be lower in the non-pressurized rig than in the engine in order to obtain the same deposition/oxide dissolution rates, and higher in order to condense a layer of the same thickness as at the turbine stagnation-point. It should be pointed out that iso-dissolution rate profiles would diverge from iso-deposition rate profiles everywhere on the blade surface except at the stagnation-point; in order to simulate the oxide dissolution characteristics of the operational turbine blade, therefore, the rig would have to reproduce the liquid layer dynamics on the blade, as well as the gas-phase dynamics.

Thus far, we have made calculations for a particular set of 'standard' test-turbine conditions ($P_o = 2.5565$ atm., $Ma_\infty = 0.4$, $T_{dp,o} = 1220K$). Generation of such simulation-graphs encompassing a wide range of engine operating conditions could be useful in arriving at an 'international-standard' rig-testing procedure.

6. CONCLUSIONS, RECOMMENDATIONS

Some interesting results of our recent studies of blade-induced alkali-salt mass-extraction from combustion gases have been:

- (1) predicted oxide dissolution rates maximize on the LE, and thereafter 'track' the salt arrival rate distribution,
- (2) computed pressure-side oxide dissolution rates are in excess of the suction-side oxide dissolution rates by many orders of magnitude for solid blades with rapid transverse heat conduction and surface temperatures not far from the local dew points,
- (3) flowing upstream condensate layers can 'spill' onto downstream regions of the blade hotter than the prevailing local dew-point; conversely, 'dry-patches' can form upstream of condensates that can flow. Streamline flow can 'shift' the condensate composition from its local 'quasi-steady' value,
- (4) rotor blade root-region addition of a second component can alter the system dew-point, freezing-point, salt deposition rate and induce BL-phase change, with obvious hot-corrosion implications, and
- (5) burner rig-testing environments are heavily dependent on the hot-corrosion simulation criteria employed; in general, equality of salt arrival rate, condensate layer thickness, and oxide dissolution rate (present work) do not lead to the same test conditions.

It is encouraging that the predictions of our model mirror 'reality' rather well- especially since, in recent years, 'hot corrosion' research seems to have moved away from seeking fundamental insights towards shorter-term empiricism. We hope that our approach of integrating a fluid-dynamical treatment of the problem with the materials-oriented philosophy of conventional corrosion research will contribute to reversing this unfortunate trend. Subject to the availability of research funding, our research plans in this area include:

- (1) improving our deliberately-simplified dissolution-model of hot-corrosion as fresh turbine data (from the field or laboratories) become available in the non-proprietary literature,
- (2) incorporating the deposition mechanisms and mixture thermodynamics of commonly encountered mixed sulfate deposits, e.g., [Ca]+[Mg]+[Na], into our CFBL-VD/ideal solution theory,
- (3) treating of transient condensate flows associated with start-up/shut-down of turbo-machinery, and
- (4) examining in closer detail the effects on localized dissolution rates of secondary flows, produced in part by surface tension gradients associated with the oxide dissolution process itself.

We believe that this program will move the turbine-community closer to a reliable means of predicting/forestalling corrosion failure of engine components caused by the deposition of molten alkali salt-solutions.

7. REFERENCES

1. ROSNER, D.E. and ATKINS, R.M., in Fouling and Slagging Resulting from Impurities in Combustion Gases, R.Bryers, ed., Engineering Foundation (New York) 1983, pp. 469-492
2. ROSNER, D.E. and SESHADRI, K., in Eighteenth Int. Symp. on Combustion, The Combustion Institute (Pittsburgh, PA), 1981, pp. 1385-1394
3. SESHADRI, K. and ROSNER, D.E., AIChE J., 30, 187 (1984)
4. ROSNER, D.E. and LIANG, B., 'Laboratory Studies of the Deposition of Alkali Sulfate Vapors from Combustion Gases Using a Flash-Evaporation Technique'

(accepted for public. in Chem. Eng. Communic.; June, 1985)

5. KOHL, F.J., SANTORO, G.J., STEARNS, C.A., FRYBURG, G.C. and ROSNER, D.E., J. Electrochem. Soc., 126 , 1054 (1979)
6. ROSNER, D.E., CHEN, B.-K., FRYBURG, G.C. and KOHL, F.J., Comb. Sci. and Tech., 20 , 87 (1979)
7. SANTORO, G.J., KOHL, F.J., STEARNS, C.A., ROSNER, D.E. and GOKOGLU, S.A., 'Experimental and Theoretical Deposition Rates from Salt-Seeded Combustion Gases of a Mach 0.3 Burner Rig', NASA TP 225 (1984); in High Temperature Corrosion , NACE-6, R.A.Rapp, ed., pp. 441-450
8. ROSNER, D.E., J. Physicochem. Hydrodynamics, 1 , 159 (1980)
9. ROSNER, D.E. and NAGARAJAN, R., 'Transport-Induced Shifts in Condensate Dew-Point and Composition in Multicomponent Systems with Chemical Reaction', Chem. Eng. Sci., 40 , 177-186 (1985)
10. GOKOGLU, S.A., CHEN, B.-K. and ROSNER, D.E., 'Computer Program for the Calculation of Multicomponent Convective Diffusion Deposition Rates from Chemically Frozen Boundary Layer Theory', NASA CR 168329 (1984)
11. GOKOGLU, S.A. and ROSNER, D.E., Int. J. Heat and Mass Transfer, 27 , 639 (1984)
12. ROSNER, D.E., GOKOGLU, S.A. and ISRAEL, R., in 'Fouling of Heat Exchange Surfaces' , R.Bryers, ed., Engineering Foundation (New York) 1983, pp. 235-256
13. CASTILLO, J.L. and ROSNER, D.E., 'Theory of Surface Deposition from a Unary Dilute Vapor-Containing Stream Allowing for Condensation within the Laminar Boundary Layer' (Chem. Eng. Sci., submitted 1985)
14. CASTILLO, J.L. and ROSNER, D.E., 'Theory of Surface Deposition from a Binary Dilute Vapor-Containing Stream Allowing for Condensation within the Laminar Boundary Layer' (in preparation, 1985)
15. CASTILLO, J.L. and ROSNER, D.E., 'Theory of Surface Deposition from Particle-Laden Dilute, Saturated Vapor-Containing Streams, Allowing for Particle Thermophoresis and Vapor Scavenging Within the Laminar Boundary Layer' (Chem. Eng. Sci., submitted, July 1985); see also: 'Nonequilibrium Theory of Surface Deposition from Particle-Laden Dilute, Condensible Vapor-Containing Streams, Allowing for Particle Thermophoresis and Vapor Scavenging Within the Laminar Boundary Layer' (prepared for submission to J. Multiphase Flow, Aug 1985)
16. ROSNER, D.E., GUNES, D. and NAZIH-ANOUS, N., Chem. Engrg. Commun., 24 , 275 (1983)
17. ROSNER, D.E. and NAGARAJAN, R., 'Vapor Deposition and Condensate Flow on Combustion Turbine Blades: Theoretical Model to Predict/Understand Some Corrosion Rate Consequences of Molten Alkali Sulfate Deposition' (prepared for journal submission, 1985)
18. ROSNER, D.E. and NAGARAJAN, R., 'Multicomponent Vapor Deposition and Condensate Flow on Combustion Turbine Blades: Theoretical Model to Predict/Understand Some Corrosion Rate Consequences of Mixed Alkali Sulfate Deposition' (prepared for journal submission, 1985)
19. ISRAEL, R. and ROSNER, D.E., Aerosol Sci. and Technol., 2 , 45 (1983)



THIN CONDENSATE LAYER DYNAMICS - ROTOR BLADES

Objectives:

- Primary Flow, and its Metal Oxide
- Dissolution Rate Consequences;
- Relation to observed hot corrosion patterns?

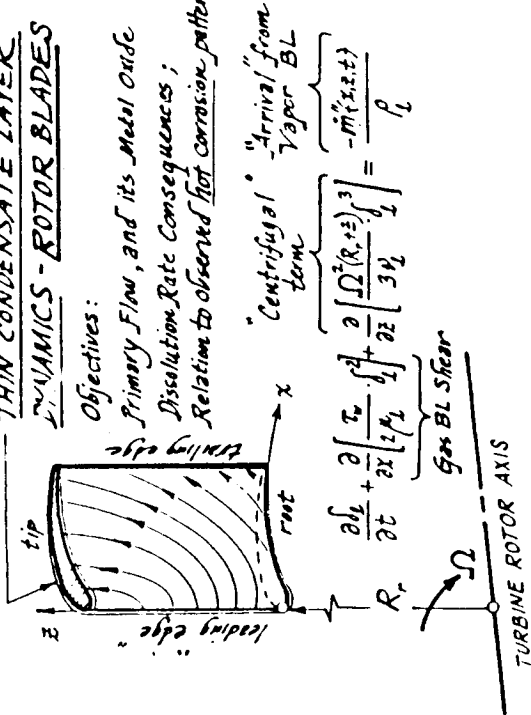


Fig. 1: Factors influencing the evolution of liquid condensate layer dynamics on a turbine rotor blade.

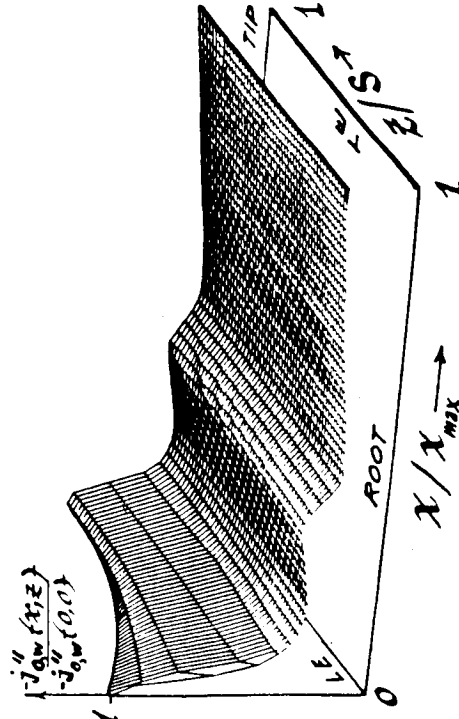


Fig. 3: Relative oxide dissolution rate distribution on suction surface of root-cooled turbine blade.

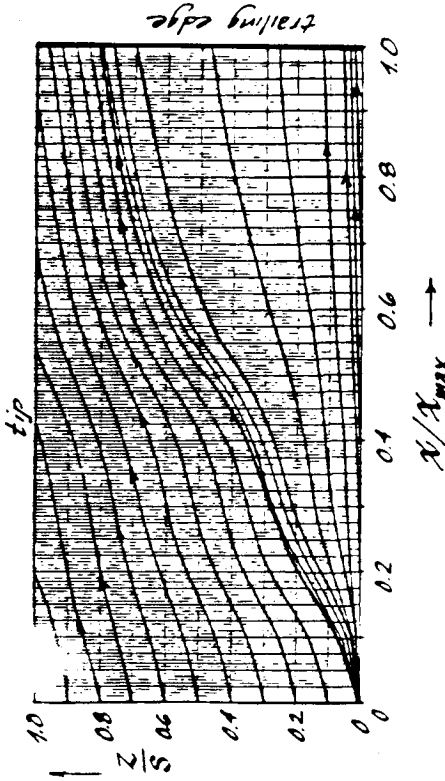


Fig. 2: Predicted streamline pattern of molten salt layer flow along suction surface of test turbine rotor blade ($\Omega = 6786$ rad/s).

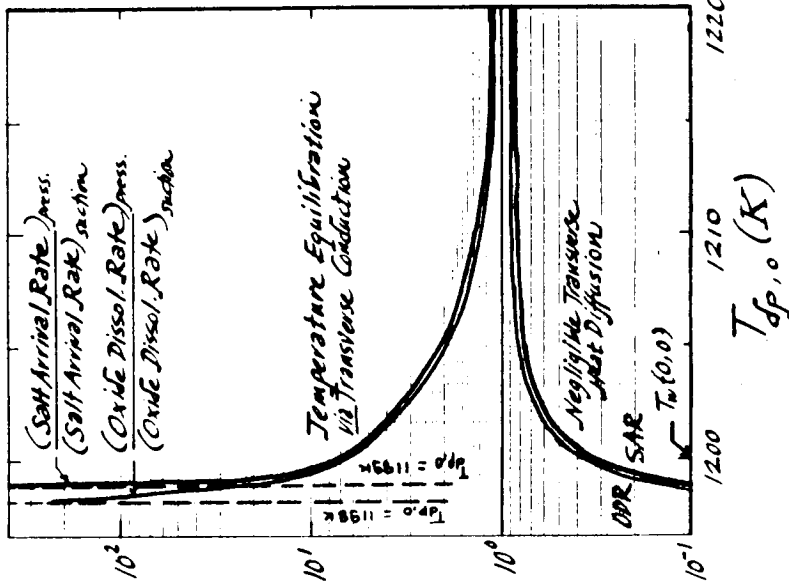


Fig. 4: Computed pressure-to-suction surface salt arrival/oxide dissolution rate ratios.

ORIGINAL PAGE IS
OF POOR QUALITY

ORIGINAL PAGE IS
OF POOR QUALITY

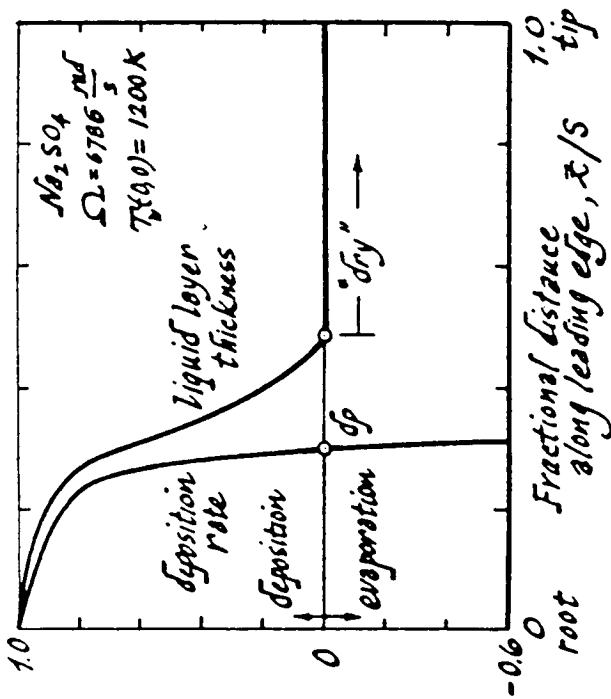


Fig. 5: Liquid layer "spill-over" onto evaporation region of rotor LE ($\Omega = 6786 \text{ rad/s}$; $T_w(0,0) = 1200\text{K}$).

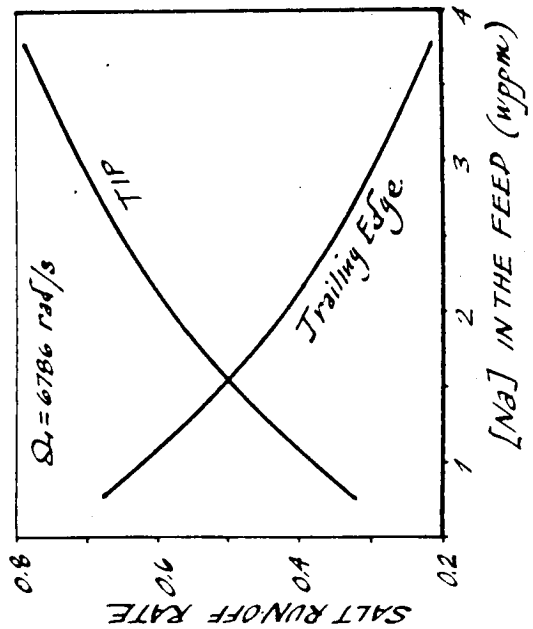


Fig. 7: Variation in salt runoff rates (TIP/TE) with salt seed level.

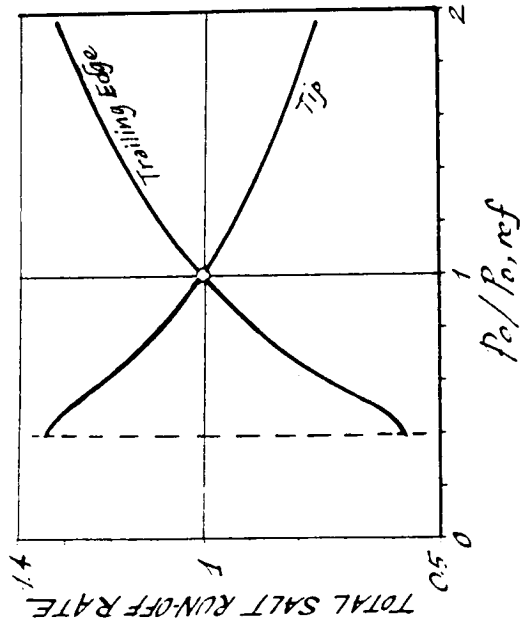


Fig. 6: Variation in salt runoff rates (TIP/TE) with stagnation pressure level.

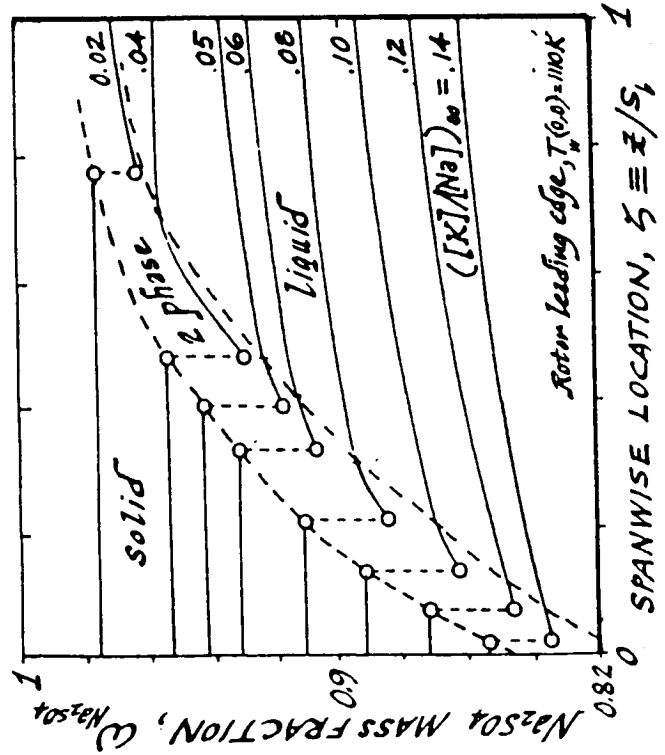


Fig. 8: Predicted distribution of condensate phase and composition of a root-cooled turbine rotor blade ($T_w(0,0) = 1110\text{K}$) vs. mainstream potassium: sodium ratio.

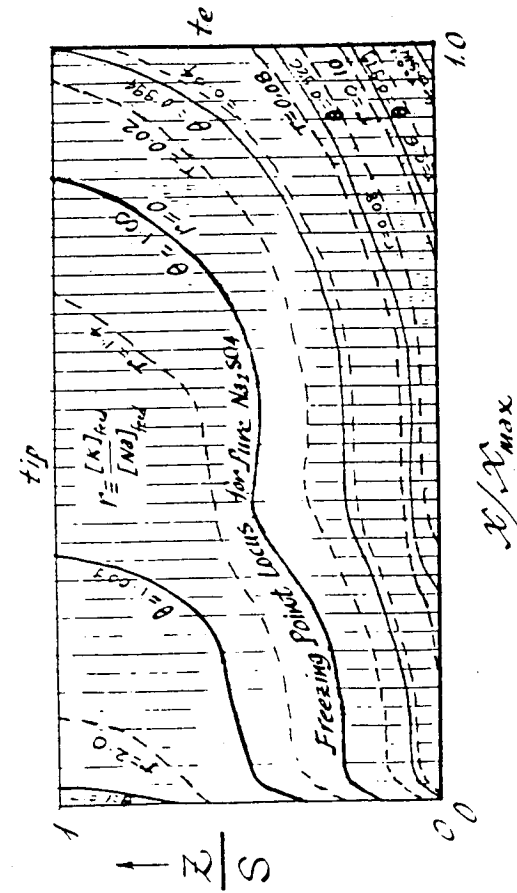


Fig. 9: Predicted distribution of liquid condensate composition on the suction surface of the rotor ($\Omega = 6786 \text{ rad/s}$; $[K]/[Na] = 0.1$).

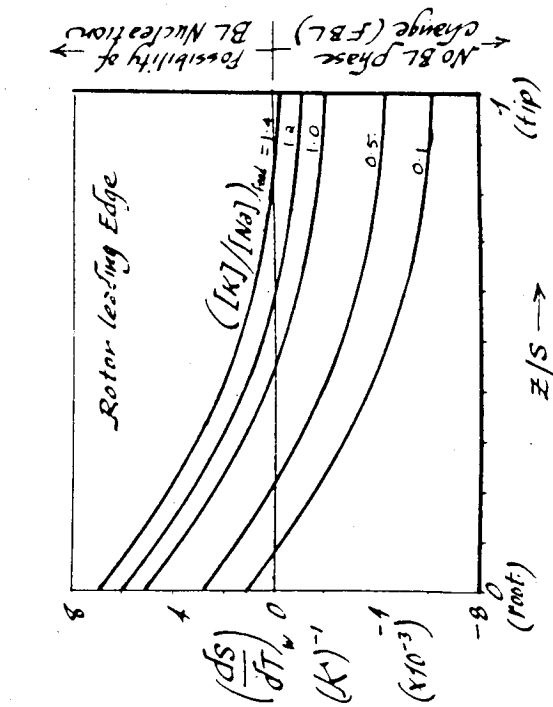


Fig. 11: Monitoring the possibility of BL-nucleation along the rotor LE as the ratio $[K]/[Na]$ in the feed changes.

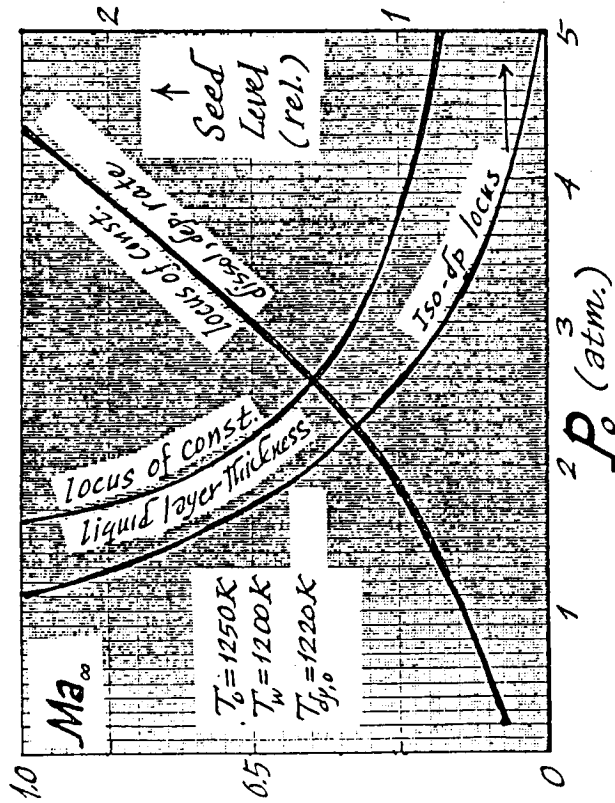


Fig. 12: Burner-rig testing under equivalent dew point conditions.